Glycolysis as a Source of "External Osmoles": The Vasa Recta Transient Model

M. Gonzalez, A.F. Hegarty, and S.R. Thomas

Abstract The kidney is one of the most important organs in our body, responsible for regulating the volume and composition of the extracellular fluid; excreting metabolic waste (as urine) and foreign substances; and also producing some hormones.

The mechanisms that contribute to the urine concentrating mechanism are not completely understood. Some ideas have been proposed over the last years and this paper is based on the hypothesis of Thomas (Am J Physiol Renal Physiol 279:468–481, 2000), that glycolysis as a source of external osmoles could contribute to the urine concentrating mechanism. Based on the steady state model developed by Thomas and also on the model developed by Zhang and Edwards (Am J Physiol Renal Physiol 290:87–102, 2005) (a model focused on microcirculation), we have developed a time-dependent model where, besides verifying some of the steady state results of Thomas (Am J Physiol Renal Physiol 279:468–481, 2000), we can also study some time dependent issues, such as the time that it will take to wash out the gradient created by glycolysis if an increase in blood inflow occurs.

1 The Kidney

In a normal human adult (Fig. 1), each kidney is about 11 cm long and about 5 cm thick, weighing 150 g. If the kidney is bisected from top to bottom, the two major regions that can be visualized are the outer *cortex* and the inner region referred as the *medulla*, where we can also distinguish two regions, the *outer medulla* (OM) and the *inner medulla*(IM).

The nephron (Fig. 2) is the functional unit of the kidney. There are more than a million in each normal adult human kidney. Each nephron contains a tuft of

A.F. Hegarty (✉)

University of Limerick, Limerick, Ireland, E-mail: alan.hegarty@ul.ie
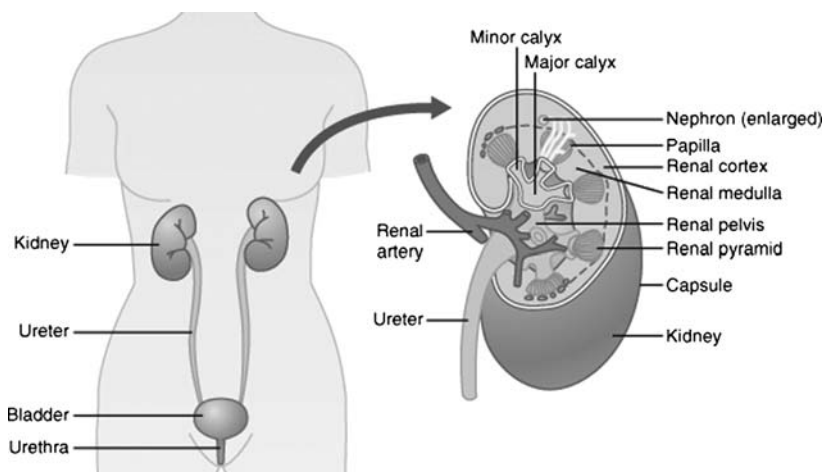
Fig. 1 Urinary system and the kidney [1]
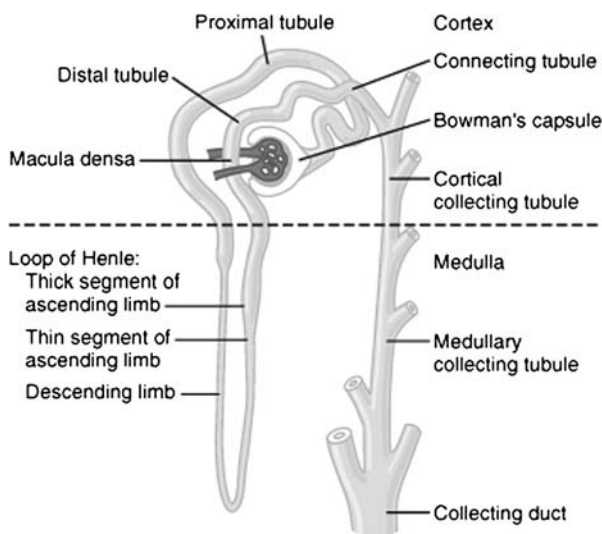
Fig. 2 Parts of the nephron [1]

capillaries called the *glomerulus*, through which large amounts of fluid are filtered from the blood, and a long *tubule* in which the filtered fluid is converted into urine on its way to the pelvis of the kidney.

Depending on how deep they lie into the medulla we can distinguish two types of nephrons: *Cortical nephrons* and *Juxtamedullary nephrons* (Fig. 4).
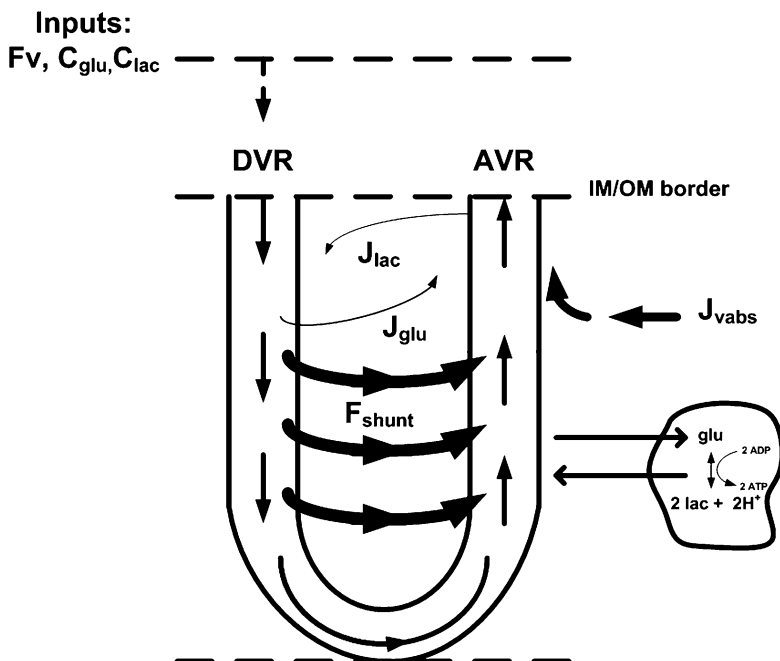
Fig. 3 Process of glycolysis in the IM cells

2 The Urine Concentrating Mechanism

Looking at urine osmolalities, mammals can produce urine that has a much higher osmolality than that of blood plasma (270–300 mOsm). This capability to concentrate their urine allows them to excrete metabolic and other waste products without compromising their water balance.

Since the 1950s, in renal physiology, the explanation for the capability of producing hypertonic urine has been a major open question. The following model was developed to study the possibility that the process of glycolysis, taking place in the IM cells (see Fig. 3) to obtain a large fraction of the energy for cell metabolism, could contribute significantly to the build-up of this gradient. During glycolysis one molecule of glucose is converted into two lactates.

3 Model Description

In the present work, a transient version of the previous paper published by Thomas [6] is developed. We consider this time the vasa recta (see Vasa Recta location in Fig. 4) and also the interstitium, where only solute movement by diffusion is considered.
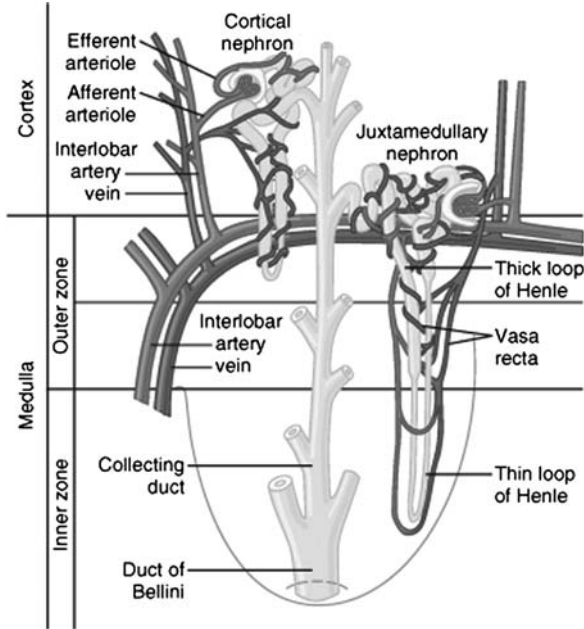
Fig. 4 Nephron blood supply showing cortical and juxtamedullary nephrons

As in previous models of the kidney we will consider a population of vasa recta represented by a single composite structure, where a fraction of the descending limb flow is shunted directly into the ascending limb at every node in the discretization where a single vasa recta turns in the inner medulla (see Fig. 3). The variable x denotes distance along the medulla, $x = 0$ at the OM/IM border and $x = L$ ($L = 4\,\text{mm}$) at the papillary tip. The numbers of DVR (descending vasa recta) and AVR (ascending vasa recta) are assumed to diminish exponentially in number along the IM toward the tip of the papilla according to the same relation as in earlier models and in conformity with reported rat anatomy:

$$N(x) = N(0)e^{-k_{sh}x} \tag{1}$$

where $N(0)$ is the number of VR at the OM/IM border. We let $N(0) = 128$ and the species dependent factor $k_{sh} = 1.213\,\text{mm}^{-1}$ which gives us a system with a single vasa recta at the papillary tip.

4 Equations

4.1 Volume Flow Equations

As in [5] we will consider the renal parenchyma indistensible, so all fluid reabsorbed flows immediately into the AVR. With such an assumptionthe equations describing

water movement are the following:

$$\frac{dF_v^d}{dx} = -J_v^d - F_{shunt} \tag{2}$$

$$\frac{dF_v^a}{dx} = -J_v^a + F_{shunt} + J_v^{ABS} \tag{3}$$

where F_v represents volume flow in descending (d) and ascending (a) vasa recta and J_v represents transmural flux of volume. As J_v depends on forces not represented in this model, we will take this as an explicit fraction ($\bar{v}$) of the entering flow.

$$J_v^d(x) = \bar{v}\frac{F_v^d(0)}{N(0)L}N(x) \tag{4}$$

$$J_v^a(x) = -J_v^d(x) \tag{5}$$

F_{shunt} is shunt transfer of volume (or solute for the equations in the next section) from DVR to AVR and is calculated as follows [10]:

$$F_{shunt}(x) = \frac{F_d(x)}{N(x)}\frac{dN(x)}{dx} \tag{6}$$

Also included in the above equations is net volume reabsorption into the AVR from LDL (long descending limb) and CD (collecting duct), designated as J_v^{ABS}.

4.2 Solute Equations

For solute flow equations we will consider the following assumptions:

1. Axial movement of solutes is by convection in the VR.
2. In the interstitium solute movement occurs by diffusion only.
3. Glucose consumed by cellular glycolysis is supplied from AVR and the resulting lactate is recovered into interstitium.
4. Interstitial cross-sectional area is taken as 40% of the total tubular luminal cross-sectional area.

Considering this we will write a PDE coupled system where we have three equations for each solute considered (glucose = g, lactate = l). As before we will use the superindexes d for DVR, a for AVR and i for interstitium equations.

$$\frac{\partial C_g^d}{\partial t} = \frac{1}{A}\left(-\frac{\partial(F_v^d C_g^d)}{\partial x} - J_g^d - F_{shunt}\right) \tag{7}$$

$$\frac{\partial C_g^a}{\partial t} = \frac{1}{A}\left(-\frac{\partial(F_v^a C_g^a)}{\partial x} - J_g^a + F_{shunt} - J_{gly}\right) \tag{8}$$

$$\frac{\partial C_g^i}{\partial t} = D_g^i \frac{\partial^2 C_g^i}{\partial x^2} + \frac{1}{A_{int}} J_g^i \tag{9}$$

$$\frac{\partial C_l^d}{\partial t} = \frac{1}{A}\left(-\frac{\partial(F_v^d C_l^d)}{\partial x} - J_l^d - F_{shunt}\right) \tag{10}$$

$$\frac{\partial C_l^a}{\partial t} = \frac{1}{A}\left(-\frac{\partial(F_v^a C_l^a)}{\partial x} - J_l^a + F_{shunt}\right) \tag{11}$$

$$\frac{\partial C_l^i}{\partial t} = D_l^i \frac{\partial^2 C_l^i}{\partial x^2} + \frac{1}{A_{int}}(J_l^i + 2J_{gly}) \tag{12}$$

where C is concentration of solute in each tube and A represents the cross-sectional area of each tube.

The relation between axial solute and axial volume flow is given by (see [9])

$$F_{ik} = F_{iv}C_{ik} - D_k\frac{\partial C_{ik}}{\partial x} \tag{13}$$

4.2.1 Membrane Flux Equations

$$J_k^j(x,t) = 2\pi r P_k(C_k^j(x,t) - C_k^i(x,t))N(x) + (1-\sigma_k)J_v(x)\frac{C_k^j(x,t) + C_k^i(x,t)}{2} \tag{14}$$

$$J_k^i(x,t) = \sum_{j=DVR,AVR} J_k^j \tag{15}$$

In (14) the first term refers to membrane diffusion (where P_k are permeabilities to glucose and lactate). The second term refers to solvent drag (where a piecewise lineralization of the Kedem–Katchalscky equation is taken [7]) and σ_k are reflection coefficients.

4.2.2 Glycolysis

Glycolytic rate is described simply with a first degree Michaelis–Menten equation saturable as a function of AVR glucose consumption

$$J_{gly}(x,t) = N(x)\frac{V_{max}C_g^a(x,t)}{K_m + C_g^a(x,t)} \tag{16}$$

4.2.3 Initial and Boundary Conditions

Flows and concentrations in the descending structures and interstitium are known at the OM/IM boundary ($x = 0$), continuity conditions are applied at the papillary tip from the ascending structures and also $(\partial C^i / \partial x)(L) = 0$. The initial concentrations throughout the tubes are set to their known values at $x = 0$.

4.3 Numerical Method

Since transmural flux of volume depends on forces not included in the model, the volume flow equations were solved analytically. The solute flow equations were solved numerically using the Method of Lines (MOL) (previously applied by Moore and Marsh [4,5]). Finite difference approximations for each of the partial derivatives with respect to the distance along the corticopapillary axis were used for the first order partial derivatives in space:

$$C_x \approx \frac{C_i - C_{i-1}}{h}, \tag{17}$$

while the second order partial derivatives were approximated with a three-point centred difference expression

$$C_{xx} \approx \frac{C_{i-1} - 2C_i + C_{i+1}}{h^2} \tag{18}$$

It might be more efficient to solve the PDE by a method specially constructed to suit the problem [2, 3], but the MOL usually enables us to solve quite general and complicated PDEs relatively easily and with acceptable efficiency. It is also attractive since powerful ODE solvers are readily available, as in our case, the ODE Matlab solver *ode15s*.

4.4 Simulations

During all simulations parameters not indicated were set as their baseline values. Twenty per cent consumption was adopted as the baseline value for glycolysis in all simulations when this is not tested. J_v^{ABS} and J_v baseline values were set at 30%.

It has been shown in previous studies [8] that $20–100\,\mathrm{mOsm/kgH_2O}$ of an unspecified external interstitial osmolytes could improve the concentration ability. Figure 5 shows different glycolysis consumptions; note that for the highest values (as was shown by Thomas [6]) the lower bound of the interval above is reached, which suggests that glycolysis should be considered in models of the urine concentrating mechanism.
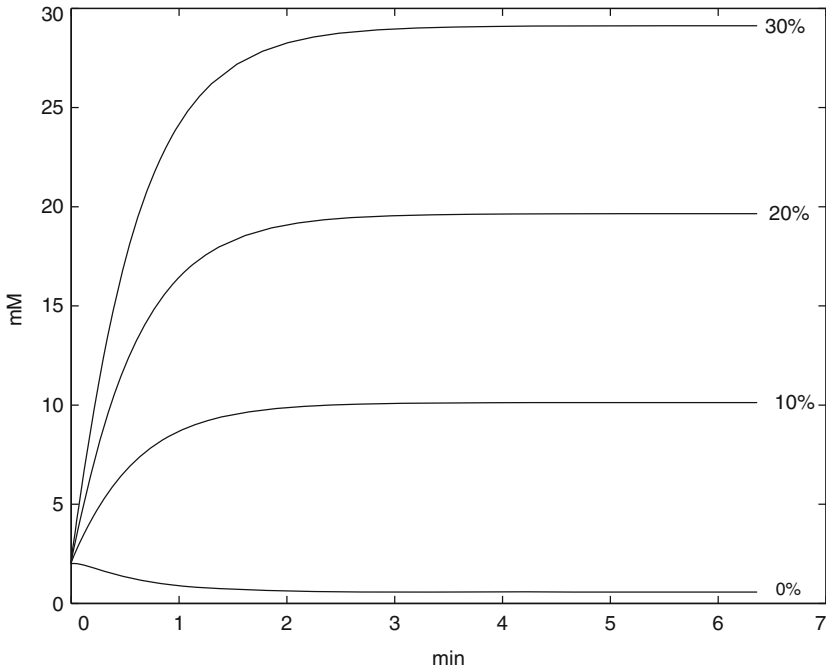
Fig. 5 The graph shows the time that it takes the lactate gradient to build up at the papillary tip for different glycolysis consumptions
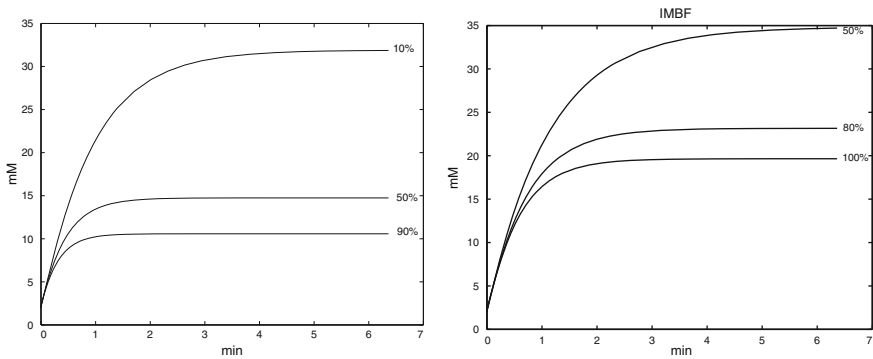
Fig. 6 *Left:* Accumulation of lactate for different volume reabsorption from nephrons at the papillary tip. *Right:* Lactate concentration when IMBF is reduced from its baseline value (absolute glucose consumption was held constant)

The effect of varying J_v^{ABS} is shown in Fig. 6. Absorption rates of 10% , 50% and 90% of DVR inflow are shown here. Increasing volume reabsorption affect significantly lactate accumulation. Also this figure shows that lactate accumulation increases dramatically as IMBF falls to one-half its baseline value, as may occur in antidiuresis. The predicted lactate profiles clearly suggest that IMBF may play an important role in the extent of lactate accumulation.
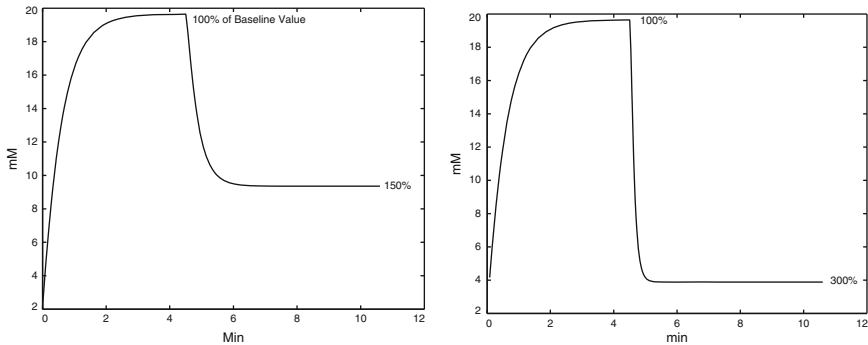
Fig. 7 Different situations of the lactate gradient being washed out after increasing IMBF at the papillary tip

Finally Fig. 7 shows different situations of the gradient being washed out after increasing the inner medullary blood flow. It can be seen that the time it takes the gradient to disappear is considerably less than the time it takes to be built up.

References

1. A.C. Guyton and J.E. Hall, *Textbook of Medical Physiology, Eleventh edition*. Elsevier Saunders, Philadelphia, 2006.
2. A.T. Layton, *A methodology for tracking solute distribution in a mathematical model of the kidney*, J. Biol. Syst. **13** (2005), 1–21.
3. A.T. Layton and H.E. Layton, *An efficient numerical method for distributed-loop models of the urine concentrating mechanism*, Math. Biosci. **181** (2003), 111–132.
4. L.C. Moore and D.J. Marsh, *How descending limb of Henle's loop permeability affects hypertonic urine formation*, Am. J. Physiol. Renal Physiol. **239** (1980), F57–F71.
5. L.C. Moore, D.J. Marsh, and C.M. Martin, *Loop of Henle during the water-to-antidiuresis transition in Brattleboro rats*, Am. J. Physiol. Renal Physiol. **239** (1980), F72–F83.
6. S.R. Thomas, *Inner medullary lactate production and accumulation: a vasa recta model*, Am. J. Physiol. Renal Physiol. **279** (2000), 468–481.
7. S.R. Thomas and D.C. Mikulecky, *Transcapillay solute exhange: a comparison of the Kedem–Katchalsky convection–diffusion equations with the rigorous nonlinear equations for this special case*, Microvasc. Res. **15** (1978), 207–220.
8. S.R. Thomas and A.S. Wexler, *Inner medullary external osmotic driving force in a 3-D model of the renal concentrating mechanism*, Am. J. Physiol. Renal Physiol. **269** (1995), F159–F171.
9. J.L. Stephenson, *Urinary concentration and dilution: models*, in Handbook of Physiology – Renal Physiology, sect. 8, vol. 2. Oxford University Press, Oxford (1992), 1349–1408.
10. A.S. Wexler, R.E. Kalaba, and D.J. Marsh, *Three-dimensional anatomy and renal concentrating mechanism. I. Modeling results*, Am. J. Physiol. Renal Physiol. **260**, (1991) F368–F383.
11. W. Zhang and A. Edwards, *A model of glucose transport and conversion to lactate in the renal medullary microcirculation*, Am. J. Physiol. Renal Physiol. **290** (2005), 87–102.